



OPEN

Effect of ultrasonic assisted EDM based on horizontal vibration on deep and small hole machining

Boting Chen¹, Menglun Tao²✉ & Zhe Luo¹✉

With the development of science and technology, industrial production requires more and more precise parts processing, precision processing has become a trend. In this trend. The traditional processing methods have been difficult to meet the market demand for micro-hole parts. Therefore, combining the characteristics of EDM and Ultrasound-assisted Machining, a new horizontal Ultrasound-assisted EDM system for deep and small holes is designed and applied in physical machining. The experimental results show that the horizontal ultrasonic vibration of workpiece can promote the efficiency and depth of EDM, and improve the electrode wear and the inner surface roughness of small holes. By comparing the processing effects of different materials, it is found that the processing efficiency and depth of pig iron are better than those of stainless steel. In conclusion, the horizontal ultrasonic vibration system established in this paper not only improves the processing effect of conventional EDM to a certain extent, but also does not affect the spindle feed and working fluid circulation of EDM machine tools. It enriches the research direction of ultrasonic assisted EDM and has broad market prospects.

Keywords Ultrasonic vibration, EDM, Amplifier, Dynamics simulation, Deep and small hole machining

When machining deep small holes with electric discharge, it is easy to generate phenomena such as arc pulling or short circuit, which accelerates electrode wear. As the processing depth increases, this disadvantage becomes particularly prominent¹. Ultrasonic assisted electrical discharge machining can greatly reduce the occurrence of such phenomena. In recent years, with the development of microfabrication technology, research on ultrasonic assisted machining has been increasingly valued.

Ultrasonic machining originated in the early 20th century, and since then, various countries have conducted research and experiments on ultrasonic machining technology. In the late 1920s, American scholars Wood and Lumis conducted ultrasonic drilling experiments using glass as the workpiece for processing. In the early 1940s, ultrasonic machining technology first appeared in relevant literature². In the mid-20th century, researchers began to apply ultrasonic vibration to electrical discharge machining processes. In 1986, Indian scholar V S. R. MURTI et al.³ studied the effect of ultrasonic radiation in machining gaps on debris in electrical discharge machining. Through scanning electron microscopy, it was found that most of the processed debris is spherical with small ellipticity. Except for some isolated hollow particles, everything else is solid. The experimental results also found that ultrasonic vibration can affect the sphericity, size, and collision rate of eroded particles. In 2015, Iranian scholars Shabgard, M. R. et al.⁴ used scanning electron microscopy and X-ray to detect the surface integrity of workpieces. The results indicate that ultrasonic vibration of cutting tools can increase normal discharge, reduce arc discharge and open circuit pulse, and thereby improve the machining quality of workpieces. In 2016, Viorel Mihai N et al.⁵ discovered that the introduction of ultrasonic vibration can improve the erosion ability of electric discharge wire cutting machining. Through a large number of experiments, the influence of different process parameters and materials on their erosion ability was obtained.

In China, ultrasonic composite processing began in the 1950s. In the late 1960s, Harbin Institute of Technology combined ultrasonic vibration with cutting to produce aluminum slender shafts with excellent cutting effects⁶.

In the early 21st century, scholar of Harbin Institute of Technology successfully developed a rotating ultrasonic processing equipment suitable for carbon fiber materials. At the same time, the Special Processing Research Institute of the school also successfully completed the development of a four axis linkage precision micro electric discharge machining machine, which can machine micro holes with diameters ranging from 8 μm to 40 μm ⁷.

Scholars Hu Jianhua et al. from Nanjing University of Aeronautics and Astronautics⁸ analyzed the influence of various parameters of ultrasonic excitation voltage on the effect of micro hole machining, and obtained a

¹College of Intelligent Manufacturing, Hunan University of Science and Engineering, 425199 Yongzhou, Hunan, P.R. China. ²School of Transportation and Logistics Engineering, Wuhan University of Technology, Wuhan 430199, P.R. China. ✉email: 185685256@qq.com; 254707121@qq.com

relationship diagram between duty cycle and machining time. Xiaopeng Yang et al. from Taiyuan University of Technology⁹ designed and analyzed the ultrasonic electric discharge machining spindle system in modules according to the different functions implemented. They designed a high-precision rotating spindle that can process ceramic coatings and efficiently and precisely process metal substrates. Through experiments, they verified the machining ability of the ultrasonic electric discharge machining process for small holes in metal based ceramic coating materials for aircraft engine turbine blades.

Tianjin University scholars Ni Hao et al.¹⁰ established a mechanical model of the ultrasonic assisted electrical discharge machining system based on the vertical vibration of electrodes, and analyzed the influence of electrode length on the resonance frequency of the system. The study showed that when using slender electrodes, the vibration system not only has the local resonance frequency of the electrodes, but also the local resonance frequency of the driving system. When the resonance frequency of the electrodes approaches and exceeds the resonance frequency of the driving system, the deviation between the resonance frequency of the system and the resonance frequency of the electrodes increases.

The paper summarizes the current research status, and attaches a ultrasonic vibration system to the workpiece. Based on the characteristics of horizontal vibration, a new type of amplitude converter is designed to meet the needs of horizontal ultrasonic assisted electrospark machining, which has certain theoretical significance and engineering value. It can be applied to the machining of various parts with deep small hole geometries.

Horizontal ultrasonic vibration and machining clearance

At present, vertical vibration is mainly applied to the machining electrode. This auxiliary machining method drives the discharge of debris inside the hole through the up and down vibration of the electrode and the cavitation effect it generates, thereby improving machining efficiency¹¹. The horizontal ultrasonic assisted machining studied in this article optimized the discharge gap of electric discharge and improved the workpiece erosion rate per discharge. Meanwhile, the cavitation effect generated by ultrasonic vibration also contributes to the removal of materials and debris, making it more practical.

Due to the fact that the surface of the workpiece is not absolutely smooth, the discharge point is always at the point with a relatively small discharge gap. When horizontal ultrasonic vibration is introduced into the workpiece, the workpiece will move back and forth under the excitation of the amplitude lever, which greatly increases the probability of spark discharge between various points on the workpiece surface and the electrode, thereby indirectly improving the discharge efficiency. The schematic diagram of horizontal ultrasonic vibration machining is shown in Fig. 1.

Assuming that the state of the electrode and the workpiece before discharge is shown in Figure (a). At this point, the breakdown gap of the electric spark is h_0 , and in Figure (a), there is only one point that meets the

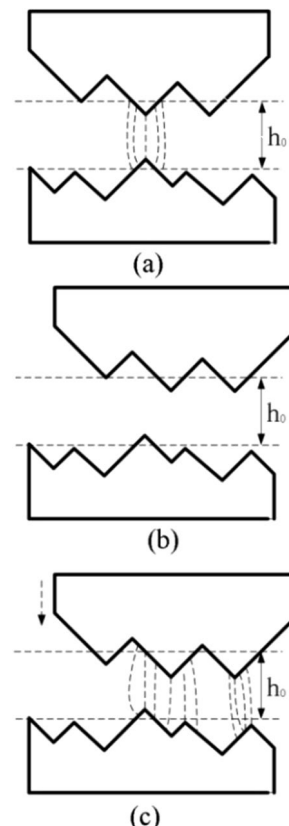


Fig. 1. Schematic diagram of horizontal vibration machining of workpieces.

requirements for electric spark breakdown. When the workpiece undergoes horizontal ultrasonic vibration, the protrusion of the electrode is misaligned with the protrusion of the workpiece. At this time, there is no point that meets the breakdown requirements, and a discharge gap cannot be formed, as shown in (b). When the machining electrode is moves downwards, the machining gap of the electric discharge decreases, and at this time, the area of the discharge channel area greatly increases, as shown in Figure (c). Therefore, horizontal ultrasonic vibration of the workpiece can improve the machining gap of electric discharge, increase the workpiece erosion rate of each discharge, and thus improve the machining efficiency of electric discharge machining.

Due to the workpiece vibration frequency is very fast, the discharge point will not stay the same area, which can greatly reduce the electrode loss. At the same time, the instability of the discharge point can also reduce the possibility of arc and short circuit.

Ultrasonic vibration system

The ultrasonic vibration system consists of three parts¹²: an ultrasonic power supply (ultrasonic generator), a transducer, and an ultrasonic amplitude converter. This paper introduces ultrasonic vibration at the processing of workpieces, and the machining schematic diagram is shown in Fig. 2:

Ultrasonic transducer

The ultrasonic vibration system designed in this paper uses a giant magnetostrictive transducer as the driving element of the amplitude converter, consisting of a shell, output shaft, GMM (Giant Magnetostrictive Material) rod, permanent magnet, and excitation coil¹³. Its basic structure is shown in Fig. 3:

The transducer uses GMM rods as the driving element, which is made of Terfenol-D (Terbium Dysprosium Iron Rare Earth Giant Magnetostrictive Alloy). The entire driving element consists of three equally long GMM rods, with permanent magnets bonded at both ends of the rods. The outer side of the driving element is the excitation coil, with a coil diameter of 0.1 mm. At the same time, apply a certain amount of prestress on the upper side of the GMM rod.

When a certain amount of current is applied to the coil, the excitation coil generates a magnetic field under the effect of the current magnetic effect. Under the action of this magnetic field, the magnetization characteristics inside Terfenol-D will change, leading to deformation. The deformation is transmitted to the amplitude lever through the output shaft, and then to the processed workpiece.

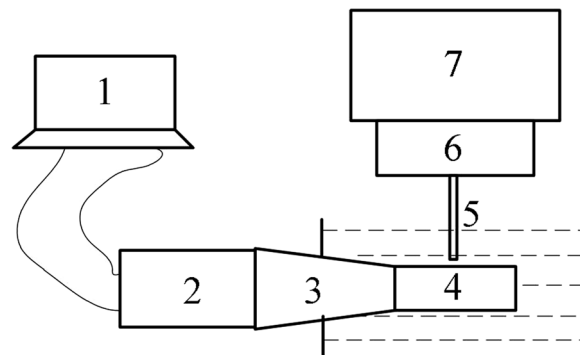
Amplitude lever

The structure of the amplitude lever is shown in Fig. 4, which is a stepped two-stage amplitude converter with a conical transition section. Among them, the cross-sectional area of the input end is S_1 , the cross-sectional area of the output end is S_3 , the cross-sectional area of the large end at the section transition is, and the cross-sectional area of the small end is S_2 . Take the section jump of the amplitude lever as the coordinate origin.

Divide the amplitude lever into sections and calculate the performance parameters of the cylindrical and conical sections in sequence. According to the solution approach of the stepped deformation amplitude pole, when $x=0$, due to the sudden change in cross-section and the complexity of the situation, the force at the sudden change can be considered continuous. Assuming that the two ends of the amplitude pole are free and the amplitude at the input end is 1, the boundary conditions are:

When $x=-a$,

$$\xi_a|_{x=-a} = 1, \frac{\partial \xi_a}{\partial x} \Big|_{x=-a} = 0 \quad (1)$$



1. Ultrasonic generator	2. Transducer
3. Amplitude lever	4. Workpiece
5. Electrode	6. Electrode rotation system
7. Pulse power supply	

Fig. 2. Ultrasonic assisted electrical discharge machining system.

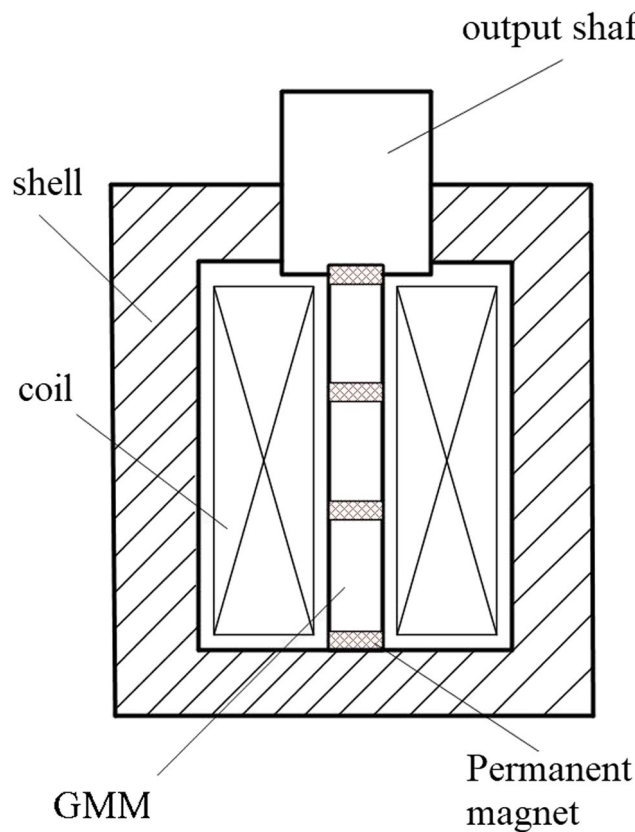


Fig. 3. Structural diagram of giant magnetostrictive transducer.

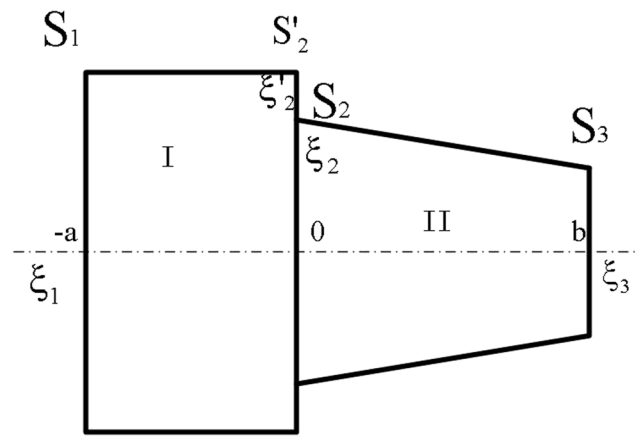


Fig. 4. Amplitude lever.

Furthermore, the displacement equation of the cylindrical segment can be obtained¹⁴:

$$\xi_a = \cos [k(a + x)] \quad (-a < x < 0) \quad (2)$$

At this point, the vibration displacement at the sudden change in cross-section:

$$\xi_2 = \xi'_{2'} = \cos (ka), \quad S_1 E \frac{\partial \xi_a}{\partial x} \Big|_{x=0} = S_2 E \frac{\partial \xi_b}{\partial x} \Big|_{x=0} \quad (3)$$

When $x=0$, $\xi_b = \xi_a$.

When $x=b$, $\xi_b|_{x=-b} = -\xi_3$.

When $0 < x < b$, the displacement equation of the conical section variable amplitude rod is¹⁵:

$$\xi_b = \frac{\alpha}{\alpha x - 1} [A\cos(kx) + B\sin(kx)] \quad (4)$$

The expression for strain distribution is:

$$\frac{\partial \xi_b}{\partial x} = \frac{\alpha}{\alpha x - 1} [-A \cdot k\sin(kx) + B \cdot k\cos(kx)] - \frac{\alpha^2}{(\alpha x - 1)^2} [A\cos(kx) + B\sin(kx)] \quad (5)$$

At this point, the constant can be determined, $A = -\frac{\cos(ka)}{\alpha}$, $B = \frac{\sin(ka) \cdot S_1}{\alpha \cdot S_2} + \frac{\cos(ka)}{k}$, The expression for particle displacement taken into Eq. (5) is¹⁶:

$$\xi_b = \frac{\cos(ka)}{1 - \alpha x} \cos(kx) - \left[\frac{S_1 \cdot \sin(ka)}{S_2 \cdot (\alpha x - 1)} + \frac{\alpha}{\alpha x - 1} \cdot \frac{\cos(ka)}{k} \right] \sin(kx) \quad (6)$$

In summary, the particle displacement equation of the amplitude lever is:

$$\begin{cases} \xi_a = \cos[k_1(a + x)] & (-a < x < 0) \\ \xi_b = \frac{\cos(ka)}{1 - \alpha x} \cos(kx) - \left[\frac{S_1 \cdot \sin(ka)}{S_2 \cdot (\alpha x - 1)} + \frac{\alpha}{\alpha x - 1} \cdot \frac{\cos(ka)}{k} \right] \sin(kx) & (0 < x < b) \end{cases} \quad (7)$$

In the above equation, $\alpha = \frac{R_1 - R_2}{R_1 L_2} = \frac{N_2 - 1}{N_2 L_2}$ ($N_2 = \frac{R_3}{R_2}$), $k = \frac{2\pi f}{c}$

(1) Resonance length

If both the cylindrical and conical sections are designed according to a 1/4 amplitude converter, the resonant length of the composite amplitude converter is:

$$L_P = L_{P_1} + L_{P_2} = \frac{\lambda}{4} + \frac{\lambda}{4} \frac{kL_2}{\pi} \quad (8)$$

(2) Displacement node x_0

Combined with the structure of the amplitude lever, it can be approximated that the displacement node is located at the center position, i.e. $x=0$.

(3) Amplification factor

when $\xi_a|_{x=-a} = 1$, $\xi_b|_{x=b} = \frac{\cos(ka)}{1 - \alpha b} \cos(kb) - \left[\frac{S_1 \cdot \sin(ka)}{S_2 \cdot (\alpha b - 1)} + \frac{\alpha}{\alpha b - 1} \cdot \frac{\cos(ka)}{k} \right] \sin(kb)$,

so the amplification factor is:

$$M_P = \left| \frac{\xi_b|_{x=b}}{\xi_a|_{x=-a}} \right| = \left| \xi_b|_{x=b} = \frac{\cos(ka)}{1 - \alpha b} \cos(kb) - \left[\frac{S_1 \cdot \sin(ka)}{S_2 \cdot (\alpha b - 1)} + \frac{\alpha}{\alpha b - 1} \cdot \frac{\cos(ka)}{k} \right] \sin(kb) \right| \quad (9)$$

(4) Calculation

The resonant frequency of the amplitude lever is known to be 12 kHz, made of 6061 aluminum alloy. The longitudinal wave velocity c in the amplitude converter is 6.1×10^6 mm/s, and the diameters of the input end (D_1), section (D_2), and output end (D_3) are 54 mm, 36 mm, and 16 mm, respectively. Therefore, the area coefficient.

$$N_2 = \frac{D_2}{D_3} = 2.25.$$

When $N_2 = 2.25$, it can be programmatically calculated that $kL_2 = 3.3351$.

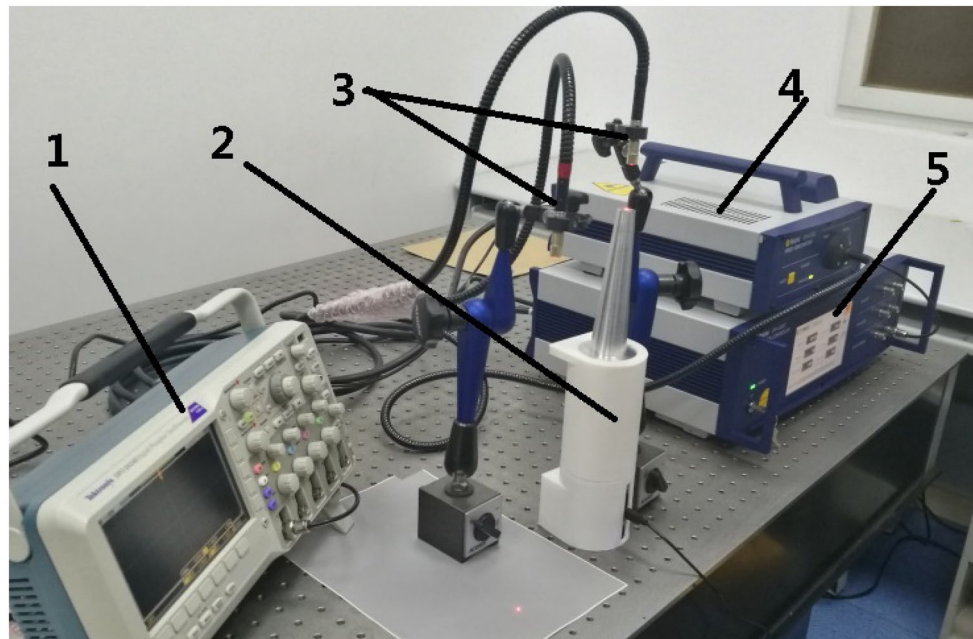
Therefore, it can be determined that the resonant length L_P of the new amplitude converter is 260 mm, with a cylindrical section length of 128 mm. Meanwhile, the amplification factor M_P of the amplitude lever is 6.9 mm, and the displacement node of the amplitude converter is located at the section mutation. In summary, the various parameters of the composite deformation amplitude pole are shown in Table 1:

In the experiment, the workbench length L_1 of the electric discharge small hole machining machine was 60 mm, and the resonance length L_P of the new amplitude lever was much smaller than half of the workbench length L_1 . Therefore, the performance parameters of the amplitude lever meet the experimental design conditions.

Amplitude verification experiment

In order to reduce the influence of external environment on experimental data and reduce experimental errors, the ultrasonic vibration system is fixed on the isolation platform and its output curve is measured using a laser

Resonance length L (mm)	Length of cylindrical segment L1 (mm)	Resonant frequency f (kHz)	Amplification factor	Amplitude (μm)
260	128	12.432	6.9	2

Table 1. Variable amplitude Pole parameters.

- 1. Digital oscilloscope
- 2. Ultrasonic vibration system
- 3. Differential laser probe
- 4. Fiber optic sensor
- 5. Laser measurement controller

Fig. 5. Measurement platform for vibration characteristics of variable amplitude rod.

signal sensor. The experimental equipment mainly includes: ultrasonic vibration system, laser signal sensor, laser vibrometer, and oscilloscope.

The measurement platform of this experiment is shown in Fig. 5, where the new amplitude converter is bonded to the end of the transducer through epoxy resin. Align one fiber optic probe of the OFV-552 fiber optic sensor with the output end of the target and the other with the connection base of the target to remove base vibration interference and obtain the relative vibration signal of the amplitude converter. In the experiment, the fiber optic probe is fixed with a magnetic gauge holder.

Results

By experiments, the displacement and velocity curves of the transducer, as well as the displacement and velocity curves of the transducer connected to the amplitude converter, can be obtained. As shown in Fig. 6:

Select a part of the curves and organize the experimental data as shown in Table 2:

In the experiment, the displacement curve measurement range of the transducer is 200 nm/V. The displacement curve measurement range of the amplitude lever is 1 μm/V. So, the output displacement of transducer is 0.28 μm, and the output displacement of Variable amplitude pole is 2 μm. Therefore the amplification factor M1 of the amplitude lever is 7.14, which is consistent with the theoretical value (6.9).

Horizontal ultrasonic assisted electrical discharge machining

This experiment was conducted on a high-speed small hole machining machine tool using electric discharge technology. The main equipment used during the experiment included a horizontal ultrasonic vibration system, an electric discharge small hole machining machine tool, and workpieces made of different materials. The electric discharge small hole machining machine tool consists of six parts: spindle, rotating head, coordinate worktable, machine electrical, control box, and working fluid system. The experimental setup is shown in Fig. 7:

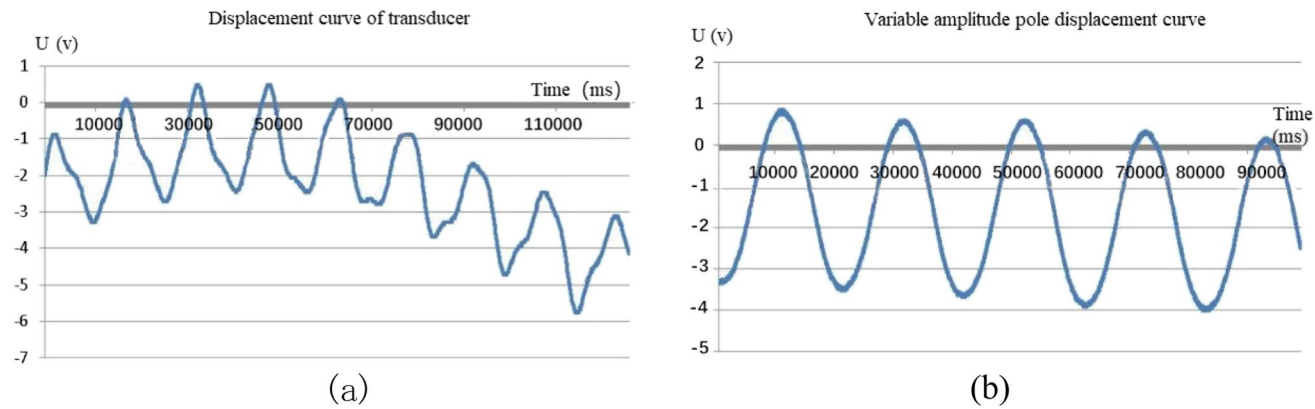


Fig. 6. Output characteristic curve of transducer and amplitude lever.

Category	Transducer	Variable amplitude pole	Category	Transducer	Variable amplitude pole
Voltage (V)	-2.4	-3.32	Voltage (V)	0.48	0.56
	-1	-1.4		-1	-1.4
	0.4	0.68		-2.32	-3.6
	-1	-1.4		-1	-1.4
	-2.24	-3.44		0.46	0.5
	-1	-1.4			
Amplitude (V)			Amplitude (V)	1.4	2

Table 2. The experimental data of vibration.

When the electric spark small hole processing machine tool starts working, the transducer is controlled to work, and the transducer transmits the displacement signal to the horn, which is amplified by the horn, so that the workpiece vibrates horizontally with the horn.

Processing speed

The experimental materials are stainless steel 304 and pig iron Z30, and their properties are shown in Table 3: The processing depth of the hole is 16mm, and the processing diameter is 2mm. The thickness of the workpiece is 16mm. Start timing when the electrode discharges, stop timing when the workpiece is perforated. The number of experimental samples is 20. After removing abnormal data caused by external environment, 16 samples are selected as experimental data for analysis, as shown in Fig. 8:

The specific values are shown in Table 4.

By calculation, it can be determined that the average speeds for conventional electrical discharge machining of stainless steel and pig iron are 0.152 mm/s and 0.139 mm/s, respectively, while the average speeds for horizontal ultrasonic assisted electrical discharge machining of stainless steel and pig iron are 0.202 mm/s and 0.205 mm/s, respectively. By comparison, it is found that under the action of horizontal ultrasonic vibration, the processing efficiency of stainless steel and pig iron has increased by 33% and 42%.

Electrode wear

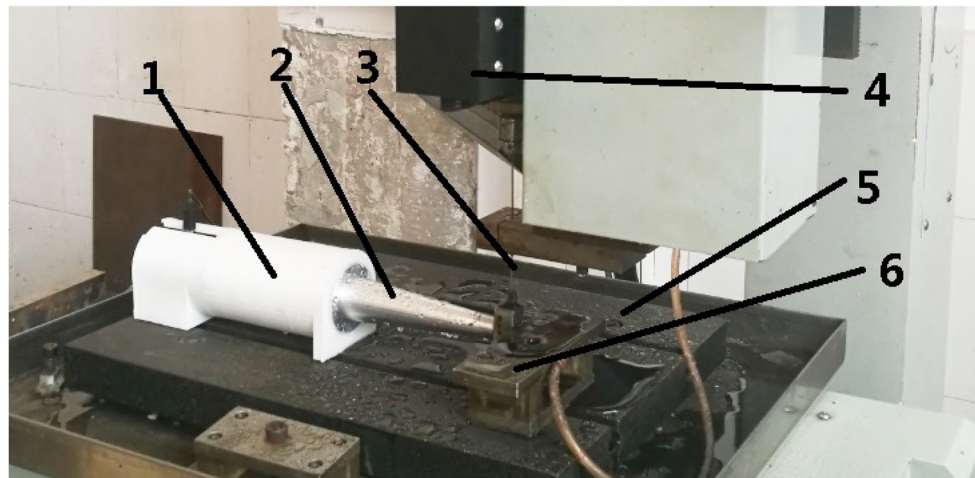
When the machining depth of the electrode is 16 mm, the wire is changed and the electrode wear data is saved. According to the above method, collect the electrode wear of horizontal ultrasonic assisted electrical discharge machining and conventional electrical discharge machining, and analyze the results. The experimental data is shown in Table 5:

As shown in the table above, when the machining depth is constant (16 mm), the average electrode wear of conventional electrical discharge machining is 5.6 mm, while the average electrode wear of horizontal ultrasonic assisted electrical discharge machining is 3.6 mm. Therefore, horizontal ultrasonic assisted electrical discharge machining can reduce electrode loss.

Take the machining electrodes of horizontal ultrasonic assisted electrical discharge machining and conventional electrical discharge machining, and observe them under a digital microscope, as shown in Fig. 9:

In Fig. 9, 1 shows the electrode wear of horizontal ultrasonic assisted electrical discharge machining, and 2 shows the electrode wear of conventional electrical discharge machining. The scale in the figure is 5000 μm .

From the picture, it can be seen that there is a serious phenomenon of secondary machining in the process of electric discharge machining. Not only will the bottom of the electrode erode the workpiece, but the side of the electrode will also react with the eroded debris, leading to severe electrode wear. Horizontal ultrasonic assisted electrical discharge machining can greatly reduce the occurrence of this phenomenon.



- 1. Ultrasonic vibration system
- 2. Variable amplitude pole
- 3. Electric discharge machining electrode
- 4. Automatic feed system
- 5. The workbench
- 6. Clamping device

Fig. 7. Horizontal ultrasonic-assisted electric discharge machining experimental device.

Material	Density	Hardness	Carbon content	Tensile strength	Melting point	Thermal conductivity
stainless steel	7.93 g/cm ³	HRB90	0.07%	520 MPa	1398°C	16.3 W/(mK)
pig iron	7.2 g/cm ³	HRB90	2.6%	800 MPa	1150°C	50 W/(mK)

Table 3. The properties of the workpiece materials.

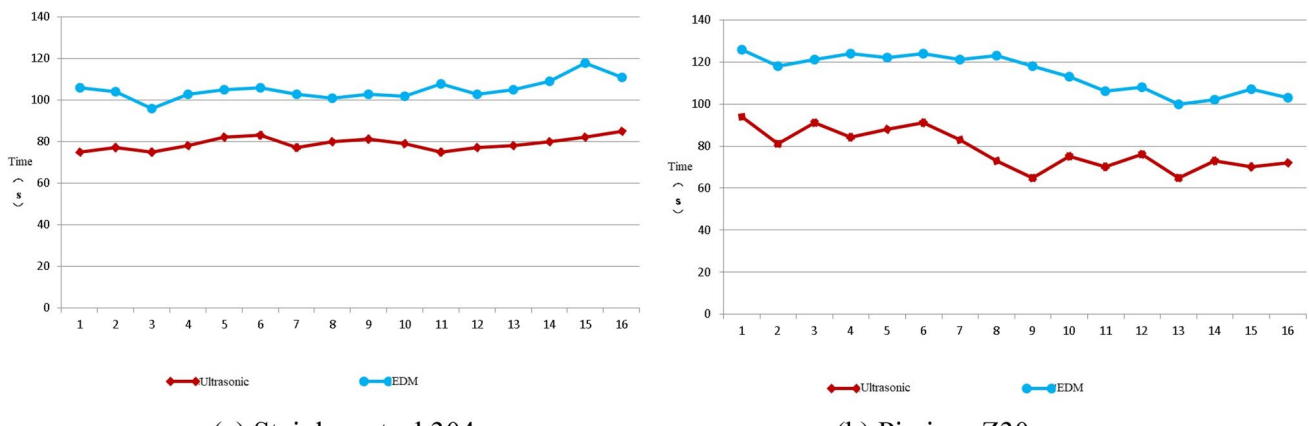


Fig. 8. Changes in efficiency of electric discharge machining with horizontal ultrasonic assistance.

When the working level vibrates, the workpiece drives the horizontal reciprocating vibration of the working fluid in the small hole, causing debris in the working fluid to accumulate towards the side wall of the small hole and be discharged with the machining fluid, thereby alleviating the wear of the electrode to a certain extent. Therefore, the electrode wear depth of conventional electrical discharge machining is higher than that of horizontal ultrasonic assisted electrical discharge machining.

Materials	Stainless steel 304				Pig iron Z30					
	Method		EDM		Ultrasonic		EDM		Ultrasonic	
Time(s)	106	103	75	81	126	118	94	65		
	104	102	77	79	118	113	81	75		
	96	108	75	75	121	106	91	70		
	103	103	78	77	124	108	84	76		
	105	105	82	78	122	100	88	65		
	106	109	83	80	124	102	91	73		
	103	118	77	82	121	107	83	70		
	101	111	80	85	123	103	73	72		

Table 4. The experimental data of processing speed.

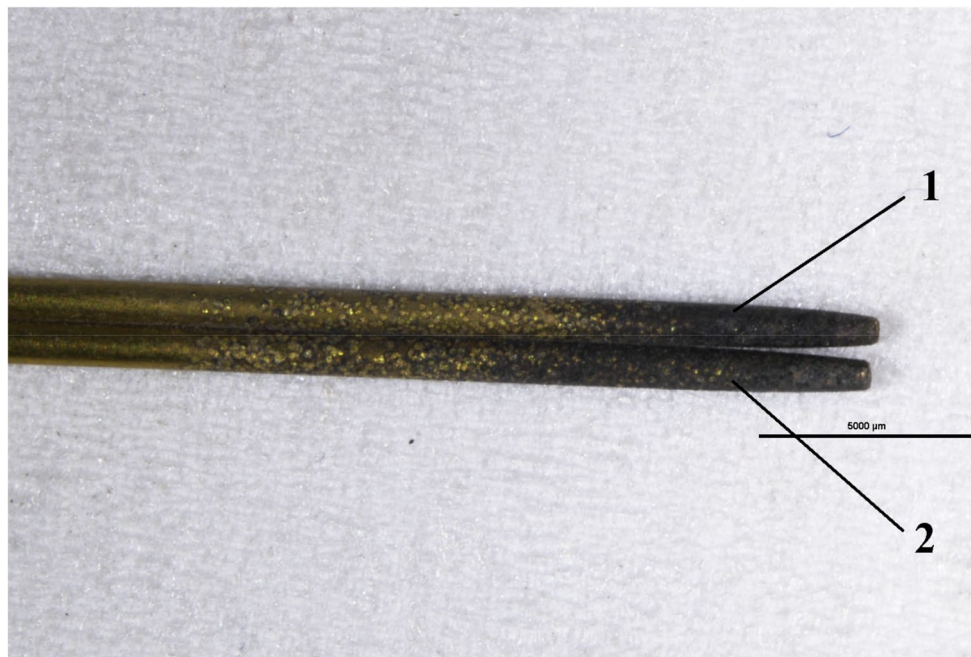
Material	Method	Initial length(mm)	Wear length(mm)				
			6	5	5	6	6
stainless steel	EDM	400	4	4	3	4	3
	Ultrasonic						

Table 5. Electrode wear under two Processing methods.

Microscopic morphology analysis

Cut the parts and select a sample that is easy to observe, clean the sample, and observe it under a digital microscope. The microstructure is shown in Fig. 10:

In Fig. 10a and b, it can be seen that in ordinary electrical discharge machining, there will be collapse phenomenon in the small holes of stainless steel, that is, the inner surface will fluctuate. It is because in the process of electric discharge machining, as the depth increases, debris deposits at the bottom and cannot be completely discharged, which affects the uniformity of discharge, leading to local overheating or burns, resulting in some large pits on the inner wall of the hole. Ultrasonic assisted machining improves the machining gap and promotes the discharge of debris due to the horizontal vibration of the workpiece. Therefore, the inner wall condition is better than that of electrical discharge machining.

**Fig. 9.** Electrode wear of two processing methods.

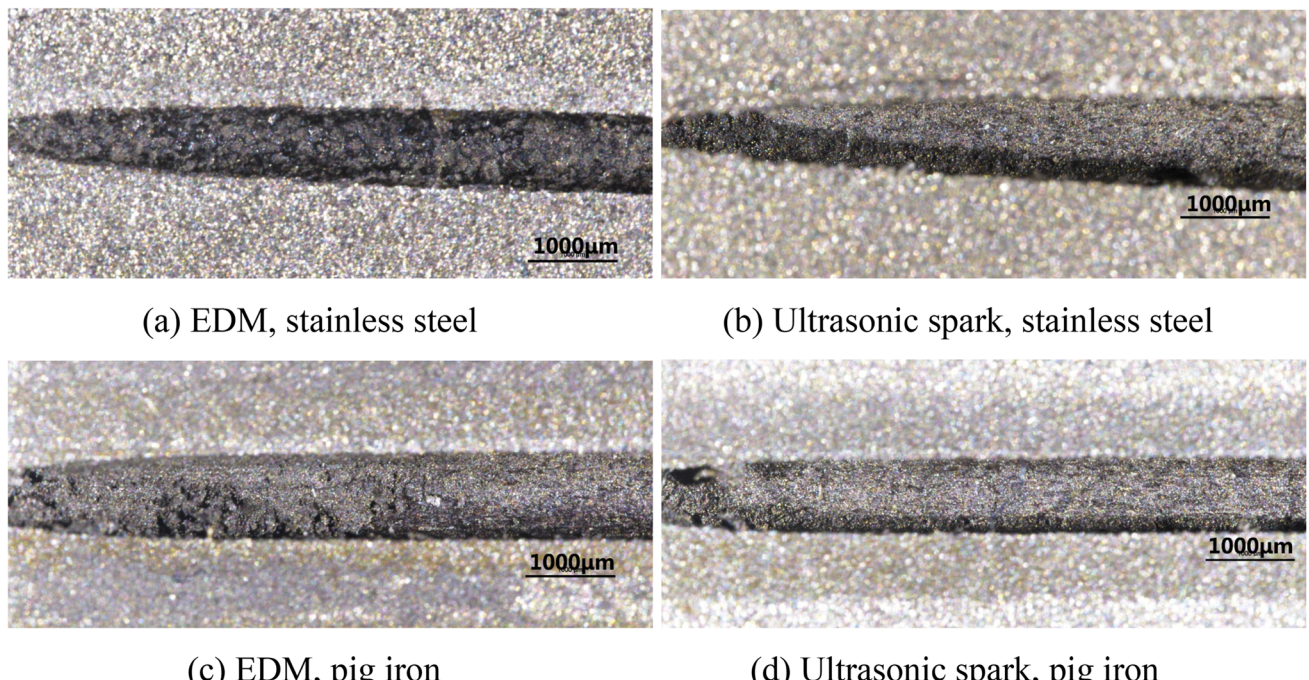


Fig. 10. Microscopic morphology of workpieces under two different processing methods.

Under the action of horizontal ultrasonic vibration, the roughness inside the hole of stainless steel (about 2 μm) is significantly higher than that of ordinary electric discharge machining (about 4 μm), and the hole is smoother, with smaller surface on the hole wall compared to ordinary electric discharge machining. Although pig iron materials also have similar phenomena, they are not obvious.

In Fig. 10c and d, the biggest difference between ordinary electric discharge machining and horizontal ultrasonic assisted electric discharge machining is the bottom of the small hole -- the surface roughness of the bottom of the small hole in ordinary electric discharge machining is lower (about 4 μm) and there is internal collapse phenomenon, but the bottom of the small hole in horizontal ultrasonic assisted electric discharge machining is relatively smooth (about 1.5 μm), and the surface inside the hole are basically melted into one piece. In summary, horizontal ultrasonic assisted electrical discharge machining can improve the internal surface roughness of small holes and avoid collapse inside the holes.

Conclusions

The paper analyzed the promoting effect of horizontal vibration of workpieces on the machining effect of electric discharge machining based on the machining mechanism of electric discharge machining. At the same time, a complete horizontal ultrasonic assisted electrical discharge machining system was established and applied in experiments, achieving the following results:

- (1) Through vibration characteristic measurement experiments, it was found that the measured value (7.1) of the amplification factor of the vibration system is close to the theoretical value (6.9).
- (2) Conducted horizontal ultrasonic assisted electrical discharge machining experiments. The experimental results indicate that horizontal ultrasonic vibration of the workpiece can improve the efficiency of electrical discharge machining. By comparison, under the action of horizontal ultrasonic vibration, the processing efficiency of stainless steel and pig iron increased by 33% and 42%, respectively. Moreover, the effect of ultrasonic vibration varies for different metal materials. For example, when processing pig iron, the processing speed of ultrasonic assisted electrical discharge machining is higher than that of stainless steel.
- (3) By comparing the degree of electrode wear and the microstructure inside the hole, it was found that under the same processing depth and material conditions, the degree of electrode wear in conventional electrical discharge machining is higher than that in horizontal ultrasonic assisted electrical discharge machining, and its degree of oxidation corrosion is deeper. By comparing the imaging images of digital stereomicroscopes with different processing materials and methods, it can be seen that the surface roughness of small holes in horizontal ultrasonic assisted electrical discharge machining is higher than that in ordinary electrical discharge machining, and there is no local collapse phenomenon inside the hole.

Data availability

All data generated or analysed during this study are included in this published article.

Received: 7 July 2024; Accepted: 28 October 2024

Published online: 15 November 2024

References

1. Ai, D. & Jia, Z. The current development status of small hole machining technology mechanical engineer (01), 8–10 (2000).
2. Xu, M. et al. Research on rotating ultrasonic assisted micro electrical discharge machining system [J]. *Mach. Tool. Hydraulic* (3), 67–70 (2016).
3. Murfi, V. S. R. & Philip, P. K. An analysis of the debris in ultrasonic-assisted electrical discharge machining [J]. *Wear.* **117** (2), 241–250 (1987).
4. Shabgard, M. R. & Alenabi, H. Ultrasonic assisted Electrical Discharge Machining of Ti 6-Al-4V Alloy[J]. *Adv. Manuf. Processes.* **30** (8), 991–1000 (2015).
5. Viorel-Mihai, N. Effect of wire electrode's ultrasonic vibration on erosive capacity to W-EDM machines [J]. *Int. J. Adv. Manuf. Technol.* **88** (1–4), 1–17 (2016).
6. Lin, J. *Microscopic Study on Ultrasonic Vibration Cutting Mechanism [D]* (Harbin Engineering University, 2000).
7. Zhenlong, W. et al. Process and experimental research on ultrasonic electric discharge machining of deep small holes in titanium alloy [J]. *Manufacturing Technology and Machine Tools* (07), 44–46+3 (2000).
8. Hu, J. & Wang, W. The influence of ultrasonic parameters on machining efficiency in ultrasonic vibration assisted electrical discharge micro hole machining [J]. *China Mechanical Engineering.* **21** (06).
9. Yang, X. *Development and Experimental Study of Ultrasonic EDM Combined Machining Spindle Device for Metal Based Ceramic Coating Materials [D]* (Taiyuan University of Technology, 2018).
10. Ni H, Gong H, Dong Y. Research on system resonance frequency in ultrasonic EDM small hole machining [J]. *Journal of Shaanxi Normal University (Natural Science Edition)* (2) (2019).
11. Zou, C. *Study on the Influence of Vertical Ultrasonic Vibration of Workpiece on Gap Flow Field in Electrical Discharge Machining [D]* (North China University, 2018).
12. Tao, J. *Micro Structure Ultrasonic Composite Electrical Machining Technology [D]* (Yangzhou University, 2010).
13. Tao, M. Research on the Theory and Implementation of Giant Magnetostrictive Materials and Device Losses 2012. Wuhan University of Technology, PhD dissertation.
14. He, X. & Gao, J. Research on the design method of ultrasonic amplitude lever [J]. *Acoustic Technology* **25**(1), 82–86 (2006).
15. Lin, Z. *The Principle and Design of Ultrasonic Amplitude Lever [M]*. (Science, 1987).
16. Shen, H., Cai, W. C. & Ding-Wen, Y. U. Design and Optimization of two-section Ultrasonic Stepped horn[J]. *J. Vib Shock* (2015).

Acknowledgements

This research was supported by the National Natural Science Foundation of China (51405357), the 2016 Hubei Province Youth Talent Development Program, 2017 Hubei Province Youth Science and Technology Morning Light Program Funding (B-class Training Visit).

Author contributions

Boting Chen wrote the main manuscript text and Zhe Luo prepared Figs. 1, 2, 3, 4, 5, 6, 7, 8, 9 and 10. All authors reviewed the manuscript.

Declarations

Competing interests

The authors declare no competing interests.

Additional information

Correspondence and requests for materials should be addressed to M.T. or Z.L.

Reprints and permissions information is available at www.nature.com/reprints.

Publisher's note Springer Nature remains neutral with regard to jurisdictional claims in published maps and institutional affiliations.

Open Access This article is licensed under a Creative Commons Attribution-NonCommercial-NoDerivatives 4.0 International License, which permits any non-commercial use, sharing, distribution and reproduction in any medium or format, as long as you give appropriate credit to the original author(s) and the source, provide a link to the Creative Commons licence, and indicate if you modified the licensed material. You do not have permission under this licence to share adapted material derived from this article or parts of it. The images or other third party material in this article are included in the article's Creative Commons licence, unless indicated otherwise in a credit line to the material. If material is not included in the article's Creative Commons licence and your intended use is not permitted by statutory regulation or exceeds the permitted use, you will need to obtain permission directly from the copyright holder. To view a copy of this licence, visit <http://creativecommons.org/licenses/by-nc-nd/4.0/>.

© The Author(s) 2024